AD-A241 003

Velocity Analysis by Inversion

by

Zhenyue Liu and Norman Bleistein

Center for Wave Phenomena
Colorado School of Mines
Golden, Colorado 80401
(303)273-3557

91-12067

91   046

Velocity Analysis by Inversion

Zhenyue Liu and Norman Bleistein

ABSTRACT

In conventional inversion methods, imaging structure inside the earth requires reasonable background velocities. In this paper, velocity analysis and structural imaging are done at the same time. The medium is assumed to consist of constant-velocity layers separated by arbitrary, smooth interfaces. The objective of the inversion is to determine layer velocities and locations of the interfaces. The velocity analysis is based on the principles that the images will be distorted when erroneous velocities are used. In particular, the difference between the depths computed by inversions from different experiments can be a measure of the error in velocity. The formulas of sensitivity to velocity error are derived for some special cases. Some computer implementations for both synthetic data and experimental data are done.

1. INTRODUCTION

Seismic data inversion process may be described as follows : given a scattered field and a background velocity, reflector maps of the earth can be constructed as singular functions of reflectors (Bleistein, 1987). The accuracy and efficiency of this method for a structural image of the earth depends largely on the complexity of the medium and on the quality and complexity of the description of background velocity. Now, we suppose that the medium is made up of constant-velocity layers separated by arbitrary smooth interfaces. Unfortunately, we have limited information from which to guess these velocities.

The inversion process is, in fact, a form of prestack depth migration. Seismic records, as input, contain information on travel time of reflected waves. Using a given velocity model, we map an image from the time domain into the depth domain. Use of incorrect background velocities generally results in a distorted image of the structure . The degree of distortion depends on the magnitude of the velocity error

and on the length scale over which signals are propagated with the initial velocity. When the velocity is correct, the image location should be at the same depth, regardless of the positions of sources and receivers, for the data used in the inversion. Otherwise, for the incorrect background velocity, the structural images for different source-receiver offsets will differ from one another. Such a deviation can help us correct the velocity. After the velocity is corrected, the interface(reflector) is determined by picking amplitudes from the output image. To guarantee a successful ray tracing which is used in the inversion code, the modeled interface must be made smooth. This process is then repeated for determining the other velocities and interface shapes for successively deeper layers.

The procedure is as follows:

(1) given an initial guess for velocity model

(2) velocity analysis on a fixed output trace to correct velocity

(3) using the correct velocity to image an interface on the output

(4) smoothing the interface

(5) repeating steps (1) to (4) for the next layer

2. MATHEMATICAL PRINCIPLES

We consider the two dimensional situation. We shall denote by X a 2-D vector, $X = (x, z)$. Let $X_s = X_s(\xi)$ be source positions and $X_r = X_r(\xi)$ be receiver positions located on the datum surface L, where ξ is a position parameter on the L. For any point below the surface, $\tau(X_s, X)$ or $\tau(X, X_r)$, respectively, denote traveltimes from X_s to X, or X to X_r.

Suppose we know the total reflection travetime $T(\xi)$. Any reflection point $X = (x, z)$ must satisfy

$$\tau(X_s, X) + \tau(X, X_r) = T(\xi). \tag{1}$$

For each ξ, the solution of equation (1) is a curve. When ξ varies, we obtain a family of curves.

Theorem 1. For any velocity function, the envelope of a solution family of equation (1) is just the reflector, $z = f(x)$, resulting in traveltime $T(\xi)$.

Proof. Differentiate equation (1) with respect to x; then

$$[\frac{\partial\tau(X_s, X)}{\partial x} + \frac{\partial\tau(X, X_r)}{\partial x}] + [\frac{\partial\tau(X_s, X)}{\partial z} + \frac{\partial\tau(X, X_r)}{\partial z}]\frac{dz}{dx} = 0. \tag{2}$$

i.e.,

$$[\nabla_X \tau(X_s, X) + \nabla_X \tau(X, X_r)] \cdot \frac{dX}{dx} = 0.$$

This is just a statement of the law of reflection. Hence the curve $z = f(x)$ is tangent to the curve family in equation (1) at every intersection point of the family of curves in (1) with the reflector. #

By the definition of an envelope, $z = f(x)$ must satisfy

$$\tau(X_s, X) + \tau(X, X_r) = T(\xi). \tag{3}$$

$$\frac{\partial \tau(X_s, X)}{\partial \xi} + \frac{\partial \tau(X, X_r)}{\partial \xi} = \frac{dT}{d\xi}. \tag{4}$$

Thus, for each ξ, we can determine the position of reflection point, (x, z), by equations (3) and (4). In general, equations (3) and (4) is hard to solve. We only conseder some special cases. Suppose that the medium velocity is a constant, c, and the datum surface L is the x-axis. Then

$$X_s = (x_s, 0), \qquad X_r = (x_r, 0), \qquad \tau(X_s, X) = \rho_s/c, \qquad \tau(X, X_r) = \rho_r/c,$$

where

$$\rho_s = \sqrt{(x_s - x)^2 + z^2}, \qquad \rho_r = \sqrt{(x_r - x)^2 + z^2}.$$

For this case, equation (3) and (4) are simplied to

$$\rho_s + \rho_r = cT(\xi), \tag{5}$$

$$\frac{\partial \rho_s}{\partial \xi} + \frac{\partial \rho_r}{\partial \xi} = cT'(\xi). \tag{6}$$

If we fix the horizontal coordinate, x, of the reflection point, then z and ξ can be considered as functions of the velocity c. Differentiating equation (5) with respect to c,

$$[\frac{\partial \rho_s}{\partial z} + \frac{\partial \rho_r}{\partial z}]\frac{dz}{dc} + [\frac{\partial \rho_s}{\partial \xi} + \frac{\partial \rho_r}{\partial \xi}]\frac{d\xi}{dc} = cT'(\xi) + T(\xi)$$

And using equation (6), we have

$$(z/\rho_s + z/\rho_r)\frac{dz}{dc} = T(\xi) = (\rho_s + \rho_r)/c.$$

Solving for dz/dc, then,

$$\frac{dz}{dc} = \frac{\rho_s \rho_r}{cz} > 0. \tag{7}$$

Introduce angles θ and ϕ as in Figure 1. Then,

$$\rho_s = z/\cos(\theta - \phi),$$

$$\rho_r = z/\cos(\theta + \phi),$$

$$\frac{dz}{dc} = \frac{z}{c\cos(\theta - \phi)\cos(\theta + \phi)}. \tag{8}$$

From (7), it follows that the imaged depth coordinate of reflection for fixed x (i.e,fixed trace location) is erroreous, when an incorrect velocity is used. Moreover, the deviation is positive when c is bigger than the true velocity ($dc > 0$), and negative
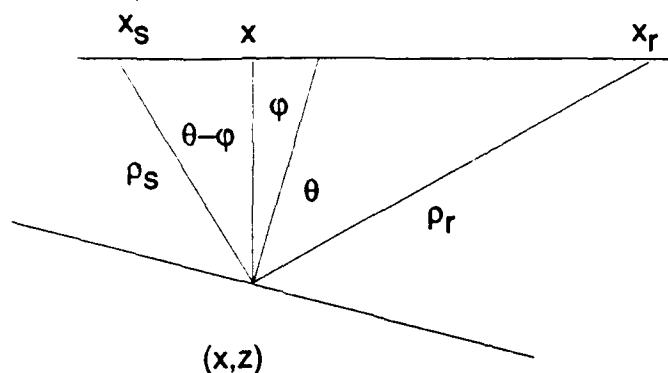
FIG. 1. Sketch of ray paths.

when c is smaller than the true velocity ($dc < 0$). Let us discuss the relationship between the deviation and the position of the source and receiver. Let c^* denote the true velocity. At $c = c^*$, z is independent of x_s and x_r. With no loss of generality, we suppose that the source is to left of the receiver, that is, $\theta > 0$.

Common-shot data

From Figure 1,

$$x_s - x = -z \tan(\theta - \phi). \qquad (9)$$

If we move from one shot point to another, i.e. x_s varies, but hold x fixed, then differentiating with respect to x_s in equation (9) yields

$$1 = \frac{-z}{\cos^2(\theta - \phi)} \frac{d\theta}{dx_s},$$

or

$$\frac{d\theta}{dx_s} = -\frac{\cos^2(\theta - \phi)}{z}. \qquad (10)$$

By differentiating (8) with respect to x_s, using equation (10), and noticing that

$$\frac{\partial z}{\partial x_s} = 0 \text{ at } c = c^*,$$

we find that

$$\frac{\partial^2 z}{\partial x_s \partial c} = -\frac{\sin 2\theta}{c \cos^2(\theta + \phi)} < 0, \text{ at } c = c^*. \qquad (11)$$

This tells us that the deviation decreases as the source moves right ($\Delta x_s > 0$).

4

Now, we will obtain error estimates in velocity analysis, which can be derived from (11). From figure 1,

$$\frac{\sin 2\theta}{x_r - x_s} = \frac{\cos(\theta + \phi)}{\rho_s} = \frac{\cos(\theta - \phi)}{\rho_r}.$$ (12)

Then (11) becomes

$$\frac{\partial^2 z}{\partial x_s \partial c} = \frac{(x_s - x_r)\,\rho_r}{c\,z\,\rho_s}, \text{ at } c = c^*.$$ (13)

Hence,

$$\frac{\partial z}{\partial x_s} \approx \frac{\partial z}{\partial x_s}\Big|_{c=c^*} + \frac{\partial^2 z}{\partial x_s \partial c}\Big|_{c=c^*}(c - c^*) = \frac{(x_s - x_r)\,\rho_r(c - c^*)}{c^*\,z\,\rho_s}.$$ (14)

Suppose that we have two shots x_{s_1}, x_{s_2} and $x_{s_1} < x_{s_2}$. Then the difference in imaged depths between the two shots can be given by

$$z(x_{s_2}) - z(x_{s_1}) \approx \frac{\partial z(x_0)}{\partial x_s}(x_{s_2} - x_{s_1}) \approx (x_{s_0} - x_{r_0})(x_{s_2} - x_{s_1})\frac{(c - c^*)}{c^*\,z}\frac{\rho_r}{\rho_s},$$

where $x_{s_0} = (x_{s_2} + x_{s_1})/2$. Thus,

$$\frac{(c - c^*)}{c^*} \approx \frac{(z(x_{s_2}) - z(x_{s_1}))\,z}{(x_{s_0} - x_{r_0})(x_{s_2} - x_{s_1})}\frac{\rho_s}{\rho_r} = \frac{\Delta z\,z}{\Delta x_s\,(x_{s_0} - x_{r_0})}\frac{\rho_s}{\rho_r}.$$ (15)

Obviously, the quotient ρ_s/ρ_r is greater than 1 for the negative dip angle, and smaller than 1 for the positive dip angle.

Relationship (15) shows us the factors that govern the accuracy of velocity analysis, $(c - c^*)/c^*$, under the assumption that medium velocity is constant. *The accuracy of velocity analysis is best for large source-to-receiver offset, well-separated shot points, and shallower target. Interestingly, it is better also for reflectors with positive dip(.i.e., receivers located in the downdip direction relative to the shot point).*

Common-offset data

Let h be half the offset. Then,

$$2\,h = z\,(\tan(\theta - \phi) + \tan(\theta + \phi)).$$

Similar to the deduction of (10), we find that

$$\frac{\partial^2 z}{\partial h\,\partial c} = \frac{2\sin 2\theta}{c\,(\cos^2(\theta + \phi) + \cos^2(\theta - \phi))} > 0, \text{ at } c = c^*.$$ (16)

Furthermore, from (12), (16) becomes

$$\frac{\partial^2 z}{\partial h\,\partial c} = \frac{2\,h}{c\,z}\frac{2\,\rho_s\rho_r}{\rho_s^2 + \rho_r^2}, \text{ at } c = c^*,$$ (17)

and

$$\frac{\partial z}{\partial h} \approx \frac{2\,h}{c^*\,z}\frac{2\,\rho_s\rho_r}{\rho_s^2 + \rho_r^2}\,(c - c^*). \tag{18}$$

Suppose that we have two offsets h_1, h_2 and $h_1 < h_2$. Then difference in imaged depths for the two offsets is given by the approximation

$$z(h_2) - z(h_1) \approx \frac{\partial z(h_0)}{\partial h}\,(h_2 - h_1) \approx 2\,h_0\,(h_2 - h_1)\,\frac{(c - c^*)}{c^*\,z}\frac{2\,\rho_s\rho_r}{\rho_s^2 + \rho_r^2},$$

where $h_0 = (h_2 + h_1)/2$. Thus,

$$\frac{(c - c^*)}{c^*} \approx \frac{(z(h_2) - z(h_1))\,z}{2\,h_0\,(h_2 - h_1)}\frac{\rho_s^2 + \rho_r^2}{2\rho_s\rho_r} = \frac{\Delta z\,z}{2\,\Delta h\,h_0}\frac{\rho_s^2 + \rho_r^2}{2\rho_s\rho_r}. \tag{19}$$

The quotient $(\rho_s^2 + \rho_r^2)/2\rho_s\rho_r$ is greater than 1 for any given dip angle.

The relationship (19) shows us that *the accuracy of velocity analysis deteriorates with increasing reflector depth and dip, and is best when the two offsets and greatly different from one another.*

Note. From (19), we can conclude that any error of velocity and the difference of the offsets result in nonzero deviation Δz. More precisely,

$$\Delta z \approx (c - c^*)(h_2 - h_1)\frac{\partial^2 z(h_0)}{\partial h\,\partial c}\,|_{c=c^*}\,.$$

Therefore, we define the quantity $\partial^2 z/\partial h\partial c$ as *the sensitivity to the velocity error.*

Multiple-layer case

If the medium is made up of more than one layer, the expression error estimate must be modified. We consider only a simple model, consisting of two horizontal layers, and consider the common-offset situationm as in Figure 2. Differentiating equation (3) with respect to c_2, and using (4), we have

$$\left(\frac{\partial\tau(X_s, X)}{\partial z} + \frac{\partial\tau(X_r, X)}{\partial z}\right)\frac{dz}{dc_2} = -\left(\frac{\partial\tau(X_s, X)}{\partial c_2} + \frac{\partial\tau(X_r, X)}{\partial c_2}\right). \tag{20}$$

For the simplicity, assume that c_1 is equal to the true value of c_2. Then, $\theta_1 = \theta_2$, and

$$\tau(X_s, X) = \tau(X_r, X) = z/c_1\cos\theta_1,$$

$$\frac{\partial\tau(X_s, X)}{\partial z} = \frac{\partial\tau(X_r, X)}{\partial z} = \frac{\cos\theta_1}{c_1},$$

$$\frac{\partial\tau(X_s, X)}{\partial c_2} = \frac{\partial\tau(X_r, X)}{\partial c_2} = \frac{-d_2}{c_1^2\cos\theta_1}.$$

From this and (20), we find that

$$\frac{dz}{dc_2}\Big|_{c_2=c_1} = \frac{d_2}{c_1\cos\theta_1{}^2}. \tag{21}$$

Furthermore, the sensitivity to the velocity error is given by

$$\frac{\partial^2 z}{\partial h\,\partial c_2}\Big|_{c_2=c_1} = \frac{d_2}{d_1+d_2}\frac{2\tan\theta_1}{c_1}, \tag{22}$$

compared to (16) (let $\phi = 0$). Equation (22) shows us that for multiple layers, *the sensitivity to the velocity error in a thin layer is reduced by the ratio of the layer thickness to layer reflector depth.*

3. SPECIAL TECHNIQUES

Iteration for velocity

If we view the depth difference Δz as a function of velocity c, then the correct velocity c^* is the one for which

$$\Delta z(c) = 0.$$

Based on this observation, we use a simple iteration to determine the velocity.

(1) Choose initial velocities c_1 and c_2 such that

$$d_1 = \Delta z(c_1) < 0, \qquad\qquad d_2 = \Delta z(c_2) > 0.$$

(2) Compute a new velocity by weighting the initial velocities as follows:

$$c_3 = c_1\,d_2/(d_2 - d_1) + c_2\,d_1/(d_1 - d_2).$$

(3) If $\Delta z(c_3) = 0$(or smaller than a given precision), the iteration will stop, with c_3 the desired velocity. If $\Delta z(c_3) > 0$, update c_3 replacing c_2 in step(1); otherwise, if $\Delta z(c_3) < 0$, update c_3 replacing c_1.

Smoothing the interface

Ray tracing in the inversion code is stable when the description of the interface has second-order smoothness. Consequently, smoothing of the interface before ray tracing is desirable.

Let $z = f(x)$ be any continuous function. We solve for a smooth function $g(x)$ that approximates $f(x)$ through the requirement

$$\int (f(x) - g(x))^2\,dx + \alpha \int (\frac{d^2g}{dx^2})^2\,dx = \min, \tag{23}$$

where $\alpha > 0$ is called the *smoothing parameter*. The larger the value of α, the smoother will be $g(x)$.

By calculus of variations we can change (23) into a differential equation for $g(x)$. For any positive number λ and any smooth function with zero boundary condition, $\eta = \eta(x)$, we define a functional,

$$B(\lambda, \eta) = \int [f(x) - (g(x) + \lambda\eta)]^2 \, dx + \alpha \int (\frac{d^2 g}{dx^2} + \lambda \frac{d^2 \eta}{dx^2})^2 \, dx.$$

Then (23) is equivalent to $\frac{dB}{d\lambda} |_{\lambda=0} = 0$, for any η. That is,

$$\int [g(x) - f(x)]\eta(x) \, dx + \alpha \int \frac{d^2 g}{dx^2} \frac{d^2 \eta}{dx^2} \, dx = 0.$$

Using integration by parts, we have

$$\int [g(x) - f(x) + \alpha \frac{d^4 g}{dx^4}]\eta(x) \, dx = 0.$$

Since η is arbitrary, this equality is satisfied if and if

$$\alpha \frac{d^4 g}{dx^4} + g(x) = f(x).$$

Taking the Fourier transform gives the solution in the wavenumber domain

$$G(k) = F(k)/(1 + \alpha k^4).$$

This expression shows that high-wavenumber components of $f(x)$ are suppressed in the approximation $g(x)$.

4. COMPUTER IMPLEMENTATIONS

To testify the efficiency of our method, we do a number of numerical common-offset experiments. The inversion code is based on the assumption that the medium is two-and-half dimensional (Hsu, 1991).

Example 1: Modeling data

First, we take synthetic common-offset data from the layered model shown in Figure 3. The input synthetic data were obtained by a common-offset modeling program. The synthetic data are generated for five gathers with common offsets 100 m, 300 m, 500 m, 700 m, and 900 m, with shots and receivers on the horizontal top surface. The first shot is at $x = 100$ m, and the shot point spacing is 20 m. Each offset uses 100 shots and receivers. The sampling interval is 4 ms, and the total reflection time is 2 sec. The inversion output spans the ranges 200 m to 1800 m in x, and 0 to 3000 m in z. Velocity analysis is done through the third layer as in Figure 6. After

8

obtaining the velocity in one layer, we pick an interface from the inversion output with this approximate velocity, then smooth it. The process is repeated recursively through all the layers. The results are as follows :

(1) In the first layer, the iterative values of c_1 are 1500, 3000, 2013; the true value is 2000.

(2) In the second layer, the iterative values of c_2 are 2013, 3500, 2863, 3022; the true value is 3000.

(3) In the third layer, the iterative values of c_3 are 3022, 4500, 4007; the true value is 4000.

Using the model consisting of these approximate velocities and interfaces, we obtain an inversion output which is very closed to the inversion output using the exact model consisting of the accurate velocities and interfaces. (See Figure 5.)

Now we test the sensitivity to velocity error. The theoretical values are computed from the equations (19) and (22). In all layers, take $\Delta c = 500\,\mathrm{m/s}$, $\Delta h = 400\,\mathrm{m}$, and $h_0 = 250\,\mathrm{m}$. In the first layer, the theoretical Δz is 100 m, the measured value is 130 m; in the second layer, the theoretical Δz is 17 m, the measured value is 30 m; in the third layer, the theoretical Δz is 12.5 m, the measured value is 10 m. The least measurable Δz (the sample spacing) is 10 m and this limits the accuracy of velocity analysis. The errors between the theoretical and measured Δz are 1/4 to 1/2 wavelength at the dominant frequency.

Example 2: Marathon data

The input data is from a physical experiment. The real medium can be approximated to a two-and-half dimensional model. The data were 296 shots, each shot with 48 receivers. The shot point spacing is 80 ft, and the receiver interval is 80 ft. We sorted the data into five gathers of common-offset with offsets 880 ft, 1680 ft, 2480 ft, 3280 ft, and 4080 ft. The first shot point is at $x = 0$. For each offset, there are 256 shots and receivers. The sampling interval is 4 ms; the total time is 2 s. The inversion output spans the ranges x from 200 to 24000 ft and z from 0 to 12000 ft. Velocity analysis is done through the fourth layer. The results are follows:

(1) In the first layer, the iterative values of c_1 are 8000, 13000, 10857, 11714; the true value is 11750.

(2) In the second layer, the iterative values of c_1 are 11714, 17000, 15679; the true value is 15750.

(3) In the third layer, the iterative values of c_1 are 15679, 24000, 21920; the true value is 22410.

(4) In the fourth layer, the iterative values of c_1 are 21920, 13000, 15973; the true value is 15750.

5. CONCLUSION

In section 4, we did computer implementations for both synthetic data and experimental data. The numerical results show that our method can obtain high accuracy in the estimate of velocity and the imaging of interface. Moreover, as a practical inversion method, there exist some questions to be stressed on.

Model limitations

The present inversion code requires that the medium be made up of constant-velocity layers separated by smooth interfaces. But, in actual subsurface, interfaces may touch each other or terminate abruptly, and velocities may vary laterally. Usually, we separate these interfaces on purpose in order to guarantee a successful inversion and assume velocities are constants. However, it will produce the model error. To solve this problem completely, a new inversion code for more general models needs to be devised.

Selection of the output trace

In theory, one output trace with a fixed horizontal coordinate is sufficient to determine the velocity. However, if the error of model cannot be ignored, such estimate of velocity may be unstable. A better way is to select more one output traces. Then take the average value of these velocities from the different traces.

ACKNOWLEDGEMENTS

REFERENCES

1. Bleistein, N., 1987, On the imaging of reflectors in the earth: Geophysics, vol. 52, 931-942.

2. Al-Yahya, Kamal, 1989, Velocity analysis by iterative profile migration: Geophysics, vol. 54, 718-729.

3. Jeannot, J. P., Faye, J. P., Dennelle, E., 1986, Prestack migration velocities from depth-focusing analysis: 56th Ann. Internat. Mtg., Soc. Expl. Geophys., Expanded Abtracts, 438-440.

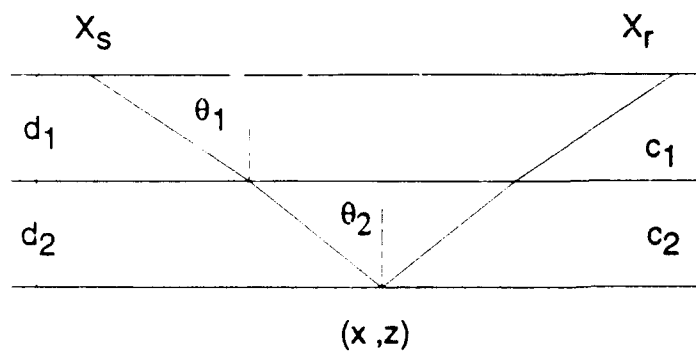4. Hsu, C., 1991, CXZCO: a common-offset inversion code: CWP Project review.
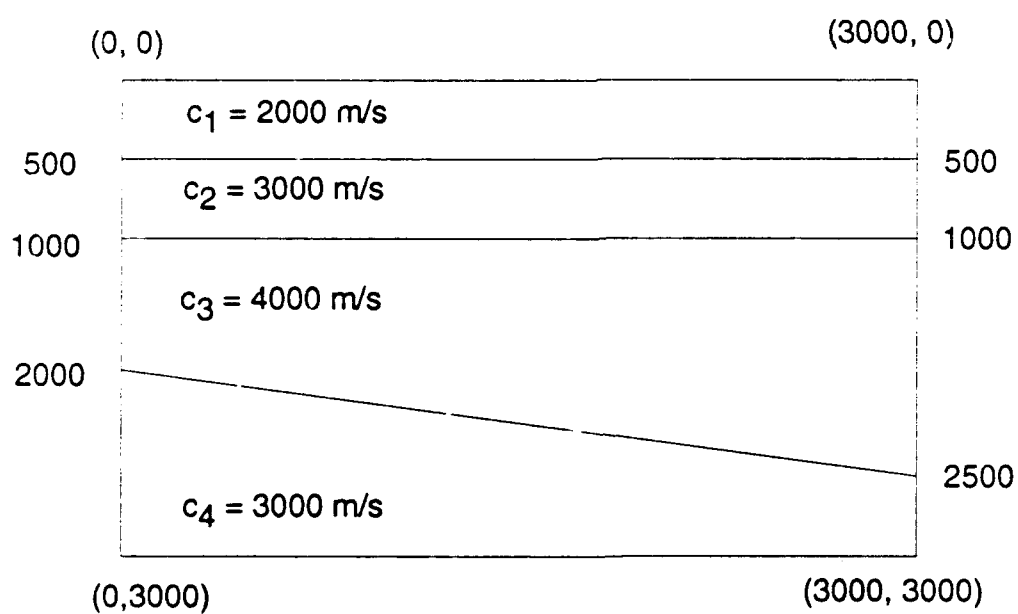
FIG. 2. Two-layer model.

FIG. 3. Test model. Lengths are in meters.

Midpoint(km) Synthetic Model

Time(sec)

Cofst Data(offset=100m)

Midpoint(km) Synthetic Model

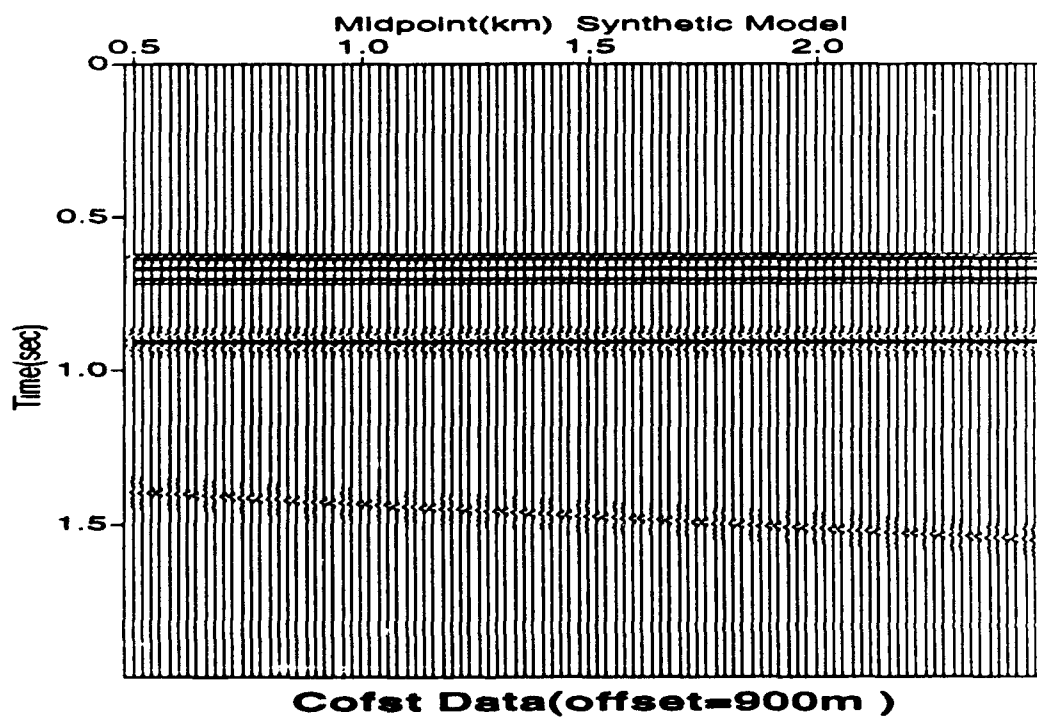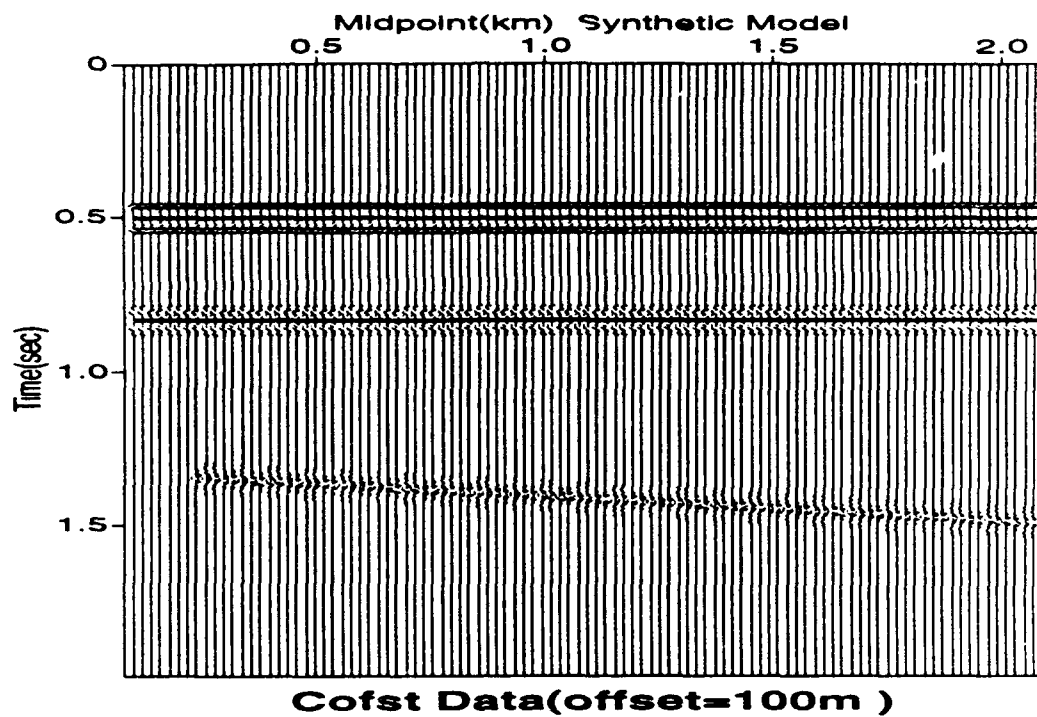**Time(sec)**

Cofst Data(offset=900m)

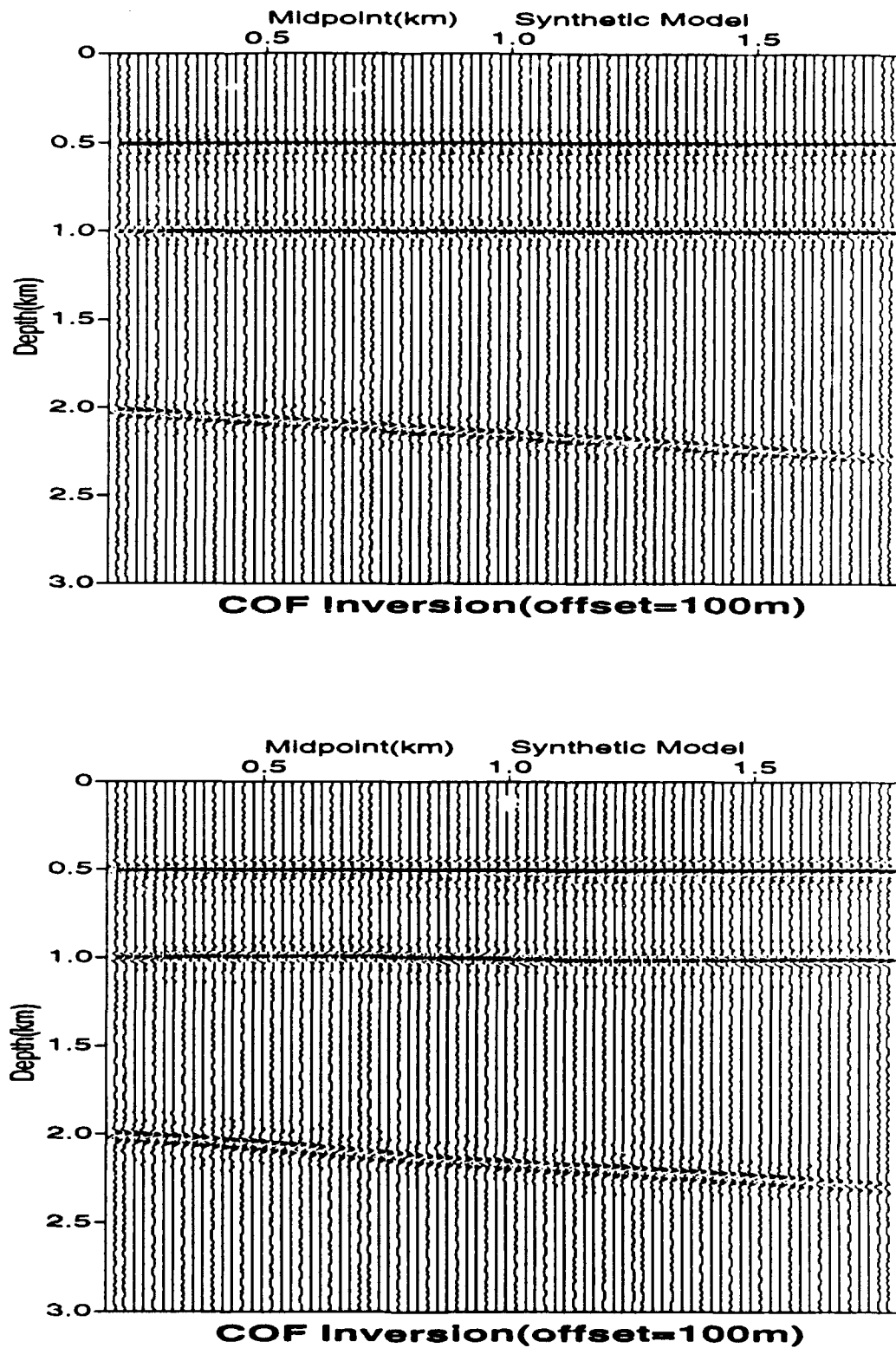FIG. 4. Input synthetic data of two offsets for the model in Figure 3.

FIG. 5. Inversion outputs. The upper uses the exact model; the lower uses the model obtained from velocity analysis.
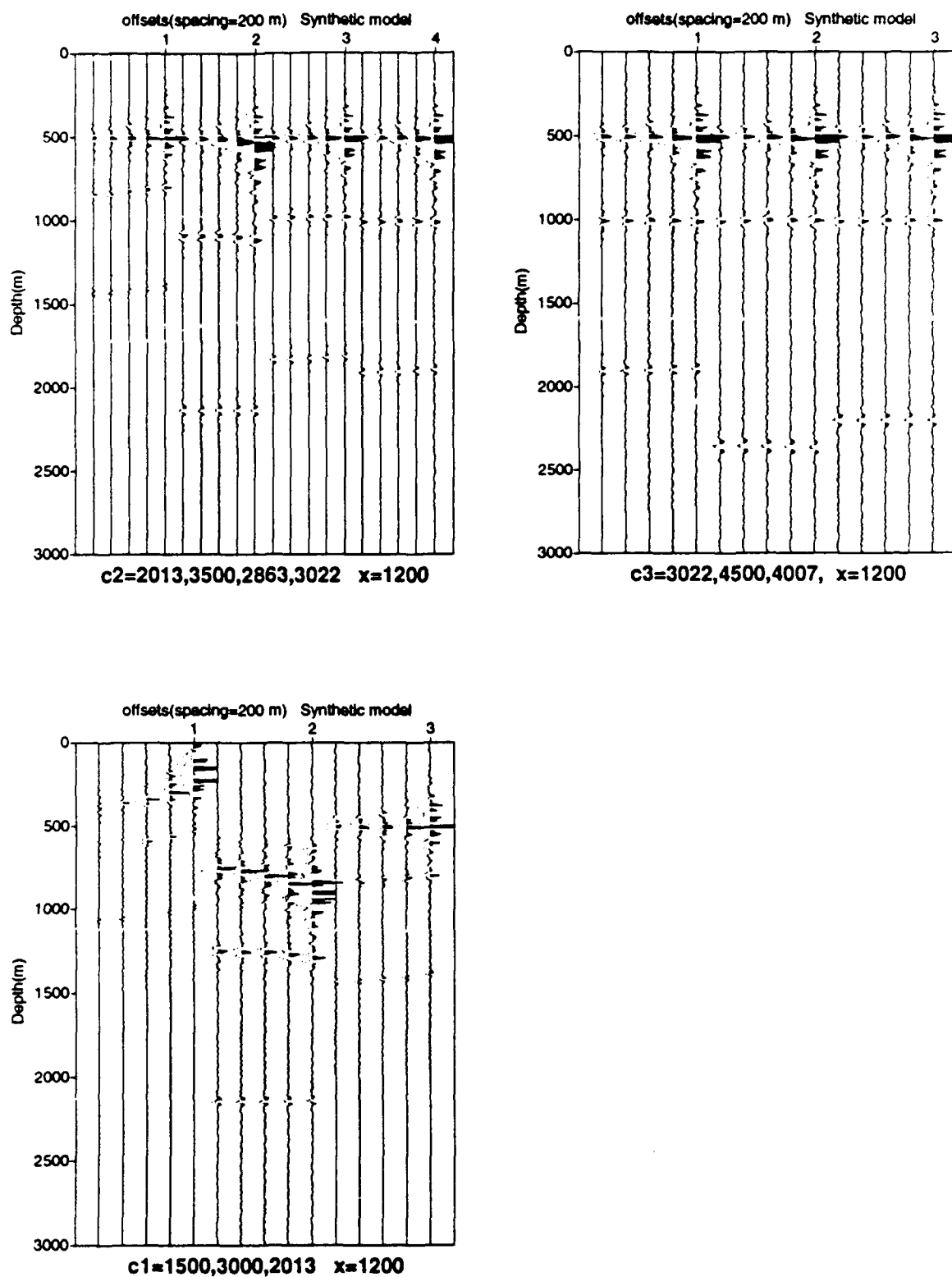
FIG. 6. Velocity analysis on the synthetic data. The true velocities: $c_1 = 2000$, $c_2 = 3000$, $c_3 = 4000$. The numbers 1, 2, 3, etc, correspond to outputs of different velocities.
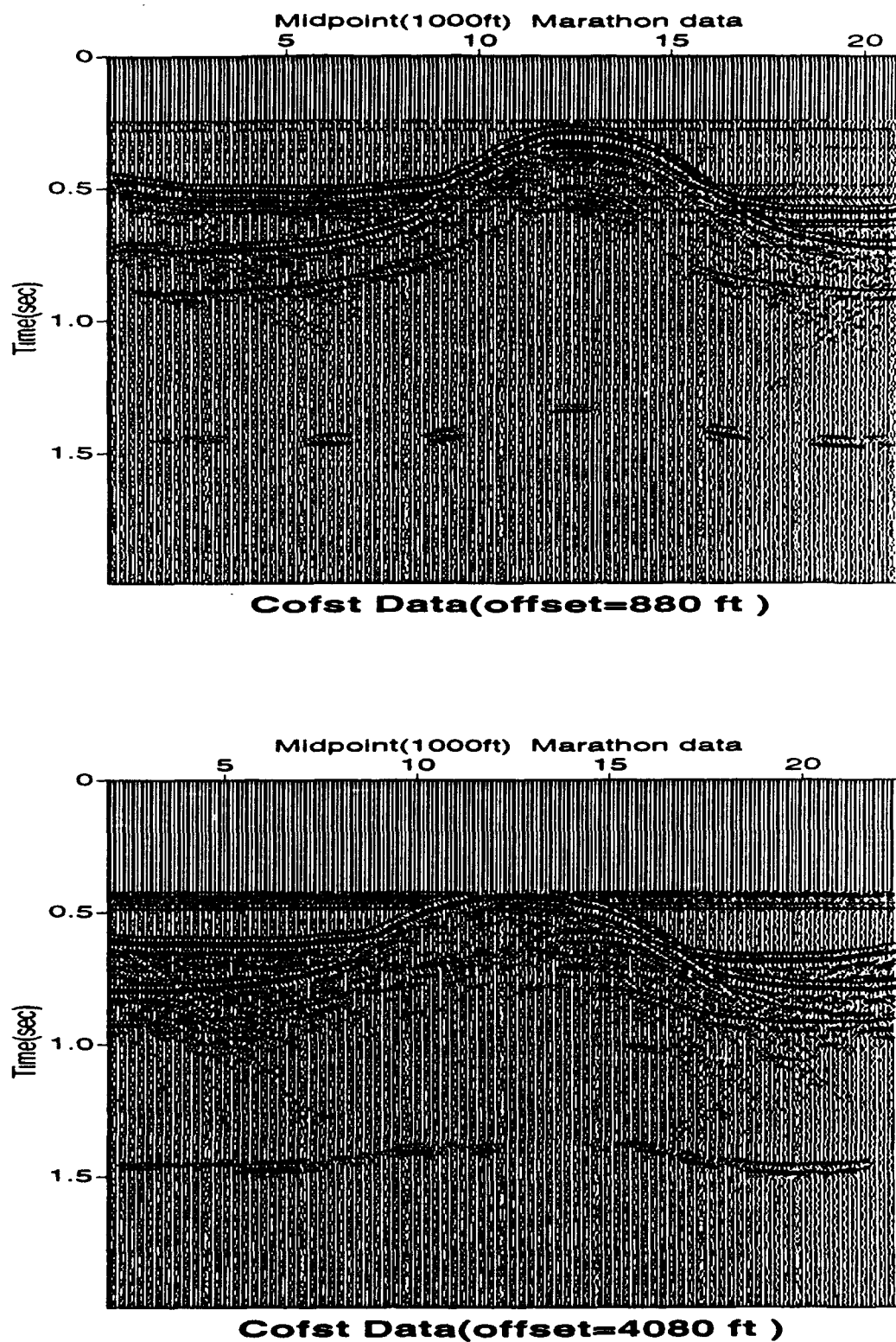
14

Cofst Data(offset=880 ft)

Cofst Data(offset=4080 ft)

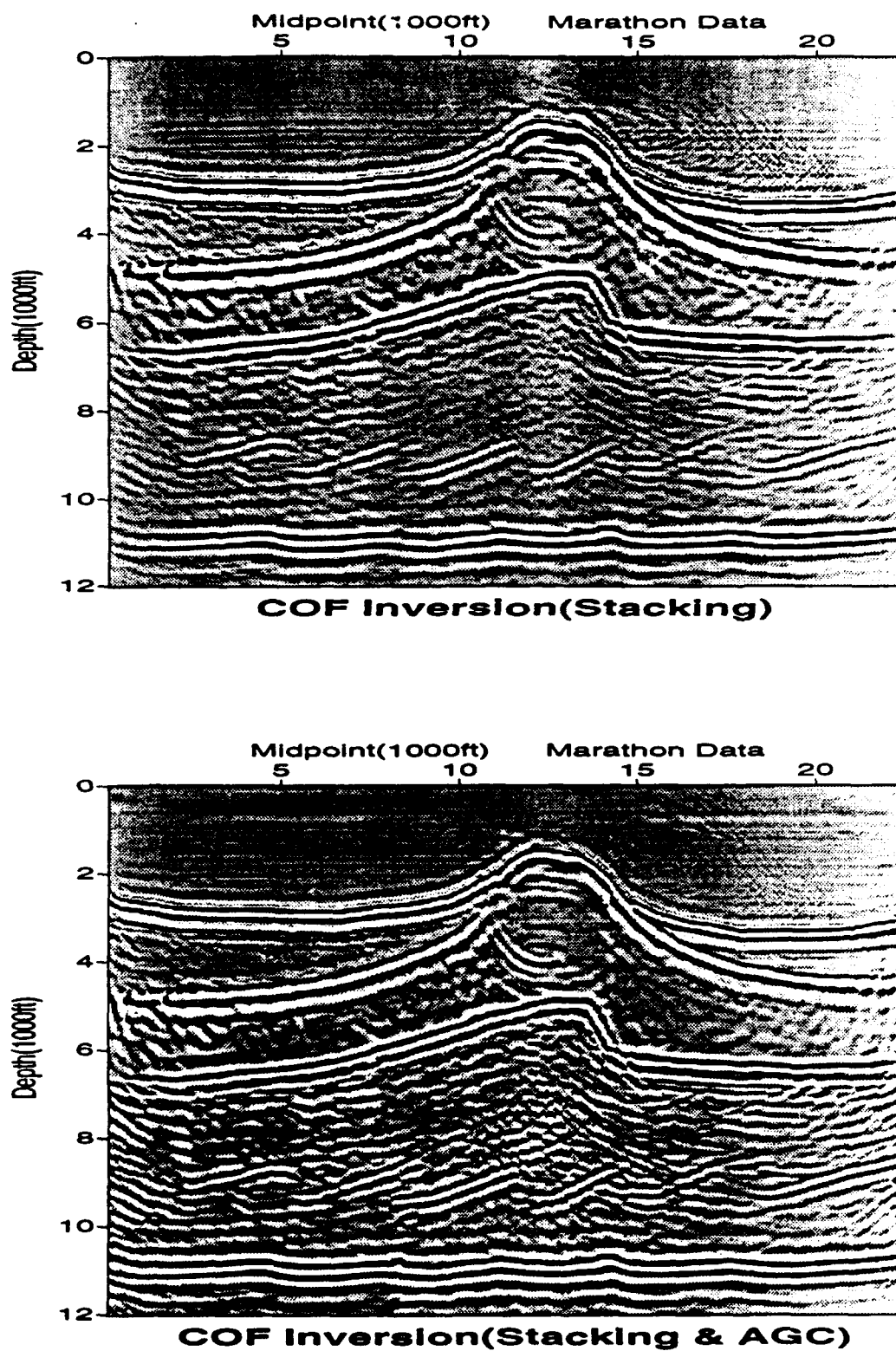FIG. 7. Model tank data for two offsets.

15

FIG. 8. Inversion outputs for the data in Figure 7. The input model was obtained from velocity analysis. Five offsets were used in the stacking.
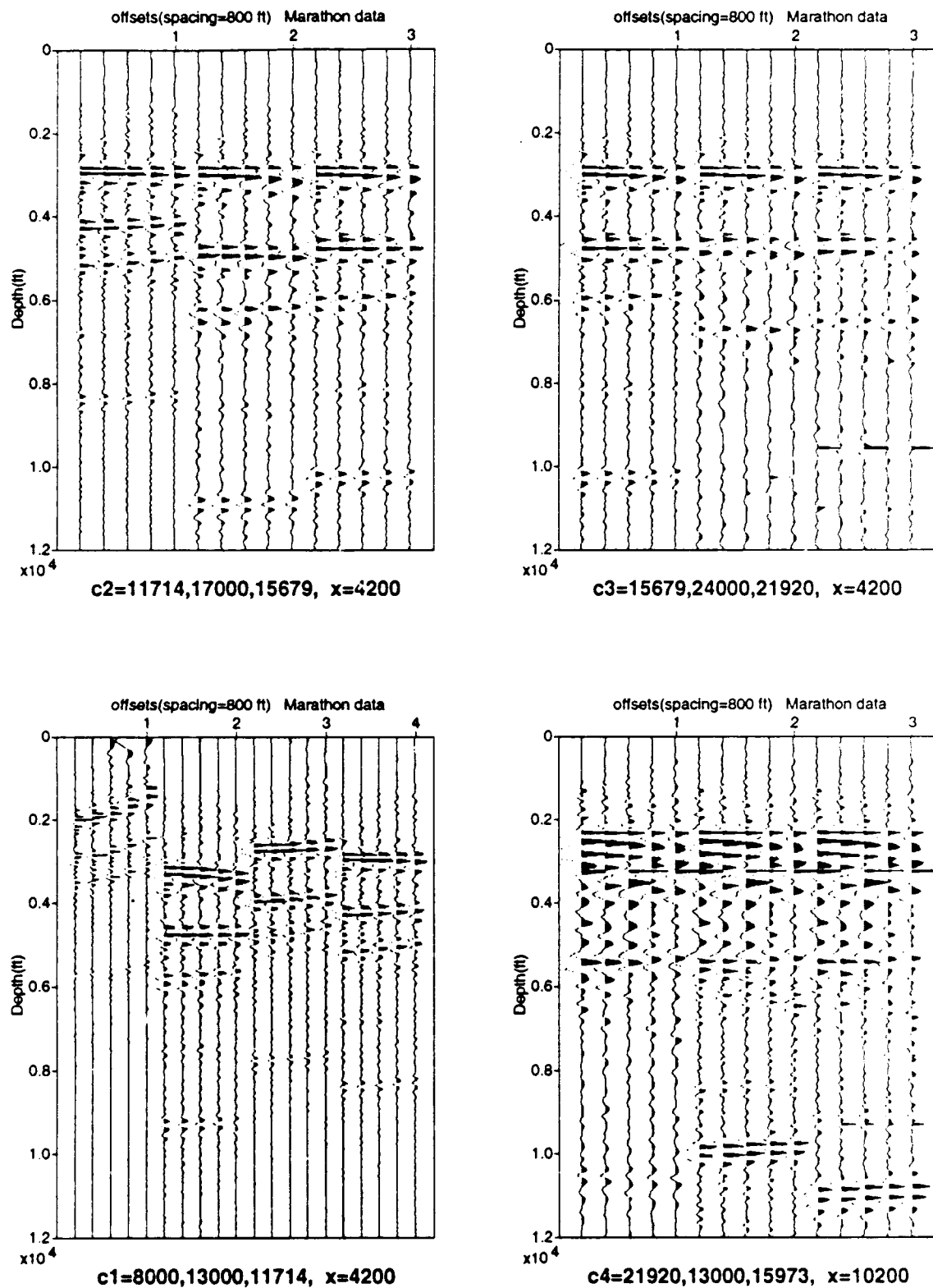
FIG. 9. Velocity analysis on the model tank data. The true velocity: $c_1 = 11750$, $c_2 = 15750$, $c_3 = 22410$, $c_4 = 15750$.

6c. ADDRESS (City, State, and ZIP Code)	7b. ADDRESS (City, State, and ZIP Code)
Golden, CO 80401	800 N. Quincy Street Arlington, VA 22217-5000

8a. NAME OF FUNDING / SPONSORING ORGANIZATION	8b. OFFICE SYMBOL (If applicable)	9. PROCUREMENT INSTRUMENT IDENTIFICATION NUMBER
		N00014-91-J-1267

8c. ADDRESS (City, State, and ZIP Code)	10. SOURCE OF FUNDING NUMBERS			
	PROGRAM ELEMENT NO.	PROJECT NO.	TASK NO	WORK UNIT ACCESSION NO.

11 TITLE (Include Security Classification)

Velocity Analysis by Inversion

12 PERSONAL AUTHOR(S)
Zhenyue Liu and Norman Bleistein

13a. TYPE OF REPORT	13b TIME COVERED	14. DATE OF REPORT (Year, Month, Day)	15 PAGE COUNT
Technical	FROM 10/1/9D TO 9/30/91	5/20/91	17

16 SUPPLEMENTARY NOTATION

17	COSATI CODES		18 SUBJECT TERMS (Continue on reverse if necessary and identify by block number)
FIELD	GROUP	SUB-GROUP	seismic modeling

19 ABSTRACT (Continue on reverse if necessary and identify by block number)

See reverse.

Abstract

In conventional inversion methods imaging structure inside the earth requires reasonable background velocities. In this paper, velocity analysis and structural imaging are done at the same time. The medium is assumed to consist of constant velocity layers separated by arbitrary, smooth interfaces. The objective of the inversion is to determine layer velocities and locations of the interfaces. The velocity analysis is based on the principles that the images will be distorted when erroneous velocities are used. In particular, the difference between the depths computed by inversions from different experiments can be a measure of the error in velocity. The formulas of sensitivity to velocity error are derived for some special cases. Some computer implementations for both synthetic data and experimental data are done.

Accesion For		
NTIS CRA&I	☑	
DTIC TAB	☐	
Unannounced	☐	
Justification		
By		
Distribution /		
Availability Codes		
Dist	Avail and / or Special	
A-1		

Statement A per telecon Dr. Lau
ONR/Code 1111MA
Arlington, VA 22217-5000

NWW 10/2/91